Annals of Mathematics and Computer Science ISSN: 2789-7206
Vol 22 (2024) 128-148 https://doi.org/10.56947/amcs.v22.287

FLOW OF MHD MICROPOLAR FLUID THROUGH POROUS MEDIUM: A HODOGRAHIC APPROACH FOR EXACT SOLUTION

SAYANTAN SIL[1*]

Abstract. An analytical study of the motion of a steady, homogenous, incompressible, plane electrically conducting micropolar fluid flow through a porous medium subjected to a transverse magnetic field is carried out. The governing non linear partial differential equations describing the continuity, momentum and angular momentum are converted into a system of linear partial differential equations by means of hodograph transformation. Further the flow equations have been obtained in terms of Legendre transform function of the stream function. Results are summarized in the form of a theorem. Lastly two examples have been taken as application to illustrate the developed theory and exact solutions are determined. The expressions for velocity, micro-rotation, streamline and pressure distribution are obtained in each case. The streamline patterns are plotted and also the pressure variation with x and y are studied for varying porous media parameter at constant density of fluid and also for varying density of different fluids at constant porous media parameter value.

1. Introduction

The study of the interaction between the moving conducting fluid and magnetic field is known as Magnetohydrodynamics (MHD). Research on MHD has become increasingly important over the years as it has got various applications in liquid metal cooling of nuclear reactors, electromagnetic casting, MHD pumps, MHD flow meters, MHD power generation among others. The liquid metal cleansing from non-metals by the use of attractive magnetic field is another basic component of application of MHD [29, 1, 28]. Also, researchers have paid lots of attention in the study and research on non-Newtonian fluids [63] as these fluids have various applications in psychology, biology, technology and industry like blood flow through arteries, vasomotion of small blood vessels, drilling of oil and gas wells, production of synthetic fibers, food stuffs, clay coating and emulsions etc.

Date: Received: Feb 28, 2024; Accepted: Mar 27, 2024.
*Corresponding Author.
2020 *Mathematics Subject Classification.* Primary 76Wxx; 76Axx; 35Cxx ; Secondary 76W05; 76S05; 35F20.

Key words and phrases. Micropolar fluid, MHD, Exact solution, hodograph transformation, micro-rotation, Legendre transform function, porous medium.

Micropolar fluids [54] are the class of fluids which show certain microscopic effects due to the local structure and microrotation of the fluid elements. In these fluids the rotation of the rigid particles which are contained in a small volume element is described by micro-rotation vector [26]. Thus, a new equation is added [11] which represent the principle of conservation of local angular momentum. This local rotation of the particles is other than the usual rigid body motion of the entire volume element [1]. In the development of the theory of the micropolar fluid credit goes to Eringen [21, 22, 20] who introduced and worked out the micropolar fluid model. The study of the flow and behavior of micropolar fluids have become prominent field of research with notable number of research papers devoted to micropolar fluid flow investigations [24, 25, 40, 70, 18, 2, 54]. In addition, study of the flow of micropolar fluid in the presence of magnetic field under various conditions and different physical parameters have been carried out by many researchers [3, 30, 62, 8, 9, 10, 13, 12, 7, 41, 31, 29, 32].

The equations governing the flow of the micropolar fluid are nonlinear and present a great deal of difficulty in solving for exact solution. Different transformation techniques are employed to transform the nonlinear equations into linear solvable form. One of such techniques is the hodograph transformation method. It consists of interchanging the dependent and independent variables in the equation to achieve linearity. In partial differential equations, if the independent variables and dependent variables are switched, then the space of independent variables is called hodograph space (in two dimensions, the hodograph plane). A curve in which the radius vector represents the velocity of a moving particle is called hodograph plane. The theory of hodograph transformation with various applications has been provided by W.F. Ames [4]. In several research papers of varied area such as gas dynamics [23, 19], viscous fluids [16], non-Newtonian fluids [51, 44], and MHD Newtonian and non-Newtonian fluid flows [65, 17] hodograph transformation method has been widely used. A large number of authors [16, 14, 5, 15, 59, 61, 66, 2, 43, 42, 56, 36, 33, 53, 34, 54, 58, 69] applied this technique to study various MHD and non-MHD fluid flows.

A porous medium consists of pores between some particulate phase, contained within a vessel or some controlled volume. In the last few decades has been of considerable interest because of ground water flows and variety of tertiary oil recovery processes. Also, there are many practical applications of fluid flow through porous medium, including filtration flow in packed column, permeation of water or oil within matrix of porous rock, cooling of electronic components, casting and welding of manufacturing processes, food processing, packed-bed reactors, storage of nuclear waste material, thermal insulation engineering, geothermal extraction, liquid metal flow through generic structures in alloy casting, and the dispersion of chemical contaminants in various processes in the chemical industry [27, 50, 56, 54]. etc. Quite a large number of research studies have been reported for the flow of fluid through porous media medium in different flow problems [46, 60, 67, 68, 6, 56, 36, 33, 37, 52, 47, 38, 53, 55, 34, 58, 45, 35, 57, 39, 48, 64].

In this paper we have considered the flow of a steady, homogenous, incompressible, plane, electrically conducting micropolar fluid through a porous medium in the presence of a transverse magnetic field. We have applied the hodograph transformation method to convert the governing non-linear system of partial differential equations into linear form. Further we have obtained the flow equations in terms of Legendre transform function of the stream function. We have considered two examples as application to illustrate the developed theory and found out exact solutions of the flow.

2. BASIC EQUATIONS

The basic equations governing the motion of steady plane flow of homogenous, incompressible, electrically conducting micropolar fluid through porous media are

$$\boldsymbol{\nabla}\cdot\mathbf{V} = 0, \tag{2.1}$$

$$\boldsymbol{\nabla}\cdot\mathbf{B} = 0, \tag{2.2}$$

$$\boldsymbol{\nabla}\times\mathbf{B} = \mu_m\mathbf{J}, \tag{2.3}$$

$$\boldsymbol{\nabla}\times\mathbf{E} = 0, \tag{2.4}$$

$$\mathbf{J}=\sigma\left(\mathbf{E}+\mathrm{V}\times\mathrm{B}\right), \tag{2.5}$$

$$\rho\left(\mathbf{V}\cdot\boldsymbol{\nabla}\right)\mathbf{V} = -\boldsymbol{\nabla}p+\kappa\left(\boldsymbol{\nabla}\times\boldsymbol{\nu}\right)-\left(\mu+\kappa\right)\boldsymbol{\nabla}\times\left(\boldsymbol{\nabla}\times\mathbf{V}\right)-\frac{\eta}{k}\mathbf{V}+\mathbf{J}\times\mathbf{B}, \tag{2.6}$$

$$\rho j\left(\mathbf{V}\cdot\boldsymbol{\nabla}\right)\boldsymbol{\nu}=\left(\alpha+\beta+\gamma\right)\boldsymbol{\nabla}\left(\boldsymbol{\nabla}\cdot\boldsymbol{\nu}\right)-\gamma\boldsymbol{\nabla}\times\left(\boldsymbol{\nabla}\times\boldsymbol{\nu}\right)+\kappa\left(\boldsymbol{\nabla}\cdot\mathbf{V}\right)-2\kappa\boldsymbol{\nu} \tag{2.7}$$

where $\mathbf{V}$ =velocity field vector, p = pressure function, $\mathbf{E}$ =electric field, $\mathbf{J}$ =current density, μ_{m} = magnetic permeability, σ =electrical conductivity of the fluid, ρ =the constant fluid field density,$\boldsymbol{\nu}$ =micro-rotation vector, η =coefficient of viscosity, k = permeability of the medium, j =micro inertia or gyration and $\mu,\kappa,\alpha,\beta,\gamma$are the material constants.
Also $\mathbf{B}$ is the total magnetic field so that $\mathbf{B}=\mathbf{B_o}$+b, $\mathbf{B}$ is the induced magnetic field, $\mathbf{B_o}$is the applied magnetic field.
The applied polarization is assumed to be zero, which implies that the electric field $\mathbf{E}$ is zero. The electric current flowing in the fluid gives rise to an induced magnetic field. In the low magnetic Reynold's number approximation, in which the induced magnetic field $\mathbf{b}$ can be ignored, the electromagnetic body force $\mathbf{J}\times\mathbf{B}$ in equation (2.2) becomes

$$\begin{aligned}\mathbf{J}\times\mathbf{B}&=\sigma\left[\left(\mathrm{V}\times\mathbf{B}_{\mathrm{o}}\right)\times\mathbf{B}_{\mathrm{o}}\right],\\ &=-\sigma\left[\mathbf{B_o}\times\left(\mathbf{V}\times\mathbf{B_o}\right)\right],\\ &=-\sigma\left[\mathbf{V}\left(\mathbf{B_o}\cdot\mathbf{B_o}\right)-\mathbf{B_o}\left(\mathbf{B_o}\cdot\mathbf{V}\right)\right],\end{aligned}$$

Also if $\left(\mathrm{B_x},\mathrm{B_y},\mathrm{B_z}\right)$are the components of the magnetic field vector $\mathbf{B}$, here the magnetic field is applied along the Z- axis, then from the solenoidal equation $\boldsymbol{\nabla}\cdot\mathbf{B} = 0$,$\mathrm{B_z}$ =constant= $\mathrm{B_o}$
Since the magnetic field is applied along the Z- axis i.e. perpendicular to the velocity field giving

$$\mathbf{B_o}\cdot\mathbf{V}=0.$$

Therefore,

$$\mathbf{J}\times\mathbf{B}= -\sigma \mathrm{B}_{\mathrm{o}}^{2}\mathrm{V},$$

If the velocity and micro-rotation components are $(u\,(x,y)\,,v\,(x,y))$and $(0,0,\Omega\,(x,y))$respectively then the governing equations (2.1), (2.6) and (2.7) takes the form as follows:

$$\frac{\partial u}{\partial x}+\frac{\partial v}{\partial y}=0\ , \tag{2.8}$$

$$\rho\left(u\frac{\partial u}{\partial x}+v\frac{\partial u}{\partial y}\right)=-\frac{\partial p}{\partial x}+\kappa\frac{\partial\Omega}{\partial y}-(\mu+\kappa)\frac{\partial\omega}{\partial y}-\frac{\eta}{k}u-\sigma\mathrm{B}_{o}^{2}\mathrm{u},, \tag{2.9}$$

$$\rho\left(u\frac{\partial v}{\partial x}+v\frac{\partial v}{\partial y}\right)=-\frac{\partial p}{\partial y}-\kappa\frac{\partial\Omega}{\partial x}+(\mu+\kappa)\frac{\partial\omega}{\partial x}-\frac{\eta}{k}v-\sigma\mathrm{B}_{\mathrm{o}}^{2}v, \tag{2.10}$$

$$\rho j\left(u\frac{\partial\Omega}{\partial x}+v\frac{\partial\Omega}{\partial y}\right)=-2\kappa\Omega+\kappa\omega+\gamma\left(\frac{\partial^{2}\Omega}{\partial x^{2}}+\frac{\partial^{2}\Omega}{\partial y^{2}}\right), \tag{2.11}$$

where $\omega\,(\mathrm{x},\ \mathrm{y})=\frac{\partial v}{\partial x}-\frac{\partial u}{\partial y}$,being the two-dimensional vorticity function.
Equations (2.8)-(2.11) form four partial differential equations four unknown functions $\mathrm{u}\,(x,y)\,,\ \mathrm{v}\,(x,y)\,,\Omega\,(x,y)\ and\ p\,(x,y)\,.$
Let us define a generalized energy function h(x, y) as:

$$h(x,y)=\frac{1}{2}\rho\left(u^{2}+v^{2}\right)+p\,, \tag{2.12}$$

also $\nabla^{2}\ =\ \partial^{2}/\partial x^{2}\ +\ \partial^{2}/\partial y^{2}$
Using the above the equations (2.9), (2.10) and (2.11) becomes

$$\frac{\partial h}{\partial x}\ =\ \rho v\omega+\kappa\frac{\partial\Omega}{\partial y}-(\mu+\kappa)\frac{\partial\omega}{\partial y}-G\mathrm{u}\ , \tag{2.13}$$

$$\frac{\partial h}{\partial y}\ =\ -\rho u\omega-\kappa\frac{\partial\Omega}{\partial x}+(\mu+\kappa)\frac{\partial\omega}{\partial x}-Gv\ \ , \tag{2.14}$$

$$\rho j\left(u\frac{\partial\Omega}{\partial x}+v\frac{\partial\Omega}{\partial y}\right)=-2\kappa\Omega+\kappa\omega+\gamma\nabla^{2}\Omega,. \tag{2.15}$$

Where,$G=\left(\frac{\eta}{k}+\sigma\mathrm{B}_{o}^{2}\right)$, is a constant.
The above system of three partial differential equations (2.13)-(2.15) along with equation (2.8) and equation for vorticity function ω contains five unknown functions u, v, $\omega\Omega$ and h as functions of (x, y) govern steady plane flows of an incompressible homogenous, electrically conducting micropolar fluid flow through a porous medium. Once a solution of these equations are found, the pressure function is determined from the expression for h(x, y) given in (2.12).

3. EQUATIONS IN HODOGRAPH PLANE

Letting the function $u=\ u\,(x,\ y)$ and $v=\ v\,(x,\ y)$ to be such that, in the region of flow, the Jacobian

$$J\,(x,y)=\frac{\partial u}{\partial x}\frac{\partial v}{\partial y}-\frac{\partial u}{\partial y}\frac{\partial v}{\partial x}\neq 0\,,\ \ |J|<\infty. \tag{3.1}$$

We may consider x and y as functions of u and v. By means of $x\ =\ x\,(u,\ v)\ \ ,y\ =\ y\,(u,\ v)\,,$ we derive the following relations:

$$\frac{\partial u}{\partial x} = J\frac{\partial y}{\partial v}\ ,\ \frac{\partial u}{\partial y} = -J\frac{\partial x}{\partial v},$$
$$\frac{\partial v}{\partial x} = -J\frac{\partial y}{\partial u}\ ,\ \frac{\partial v}{\partial y} = J\frac{\partial x}{\partial u}\ . \tag{3.2}$$

We also obtain the relations

$$\frac{\partial g}{\partial x} = \frac{\partial(g,y)}{\partial(x,y)} = \bar{J}\frac{\partial(g,y)}{\partial(u,v)}\ ,\ \frac{\partial g}{\partial y} = -\frac{\partial(g,x)}{\partial(x,y)} = \bar{J}\frac{\partial(x,g)}{\partial(u,v)}\ . \tag{3.3}$$

(**??**)Where g = g(x, y) = g(x(u, v), y(u, v)) = g(u, v) is any continuously differentiable function and

$$J = J(x,y) = \frac{\partial(u,v)}{\partial(x,y)} = \left[\frac{\partial(x,y)}{\partial(u,v)}\right]^{-1} = \bar{J}(u,v). \tag{3.4}$$

Employing these transformation relations for the first order partial derivatives and the transformation equations for the functions $\boldsymbol{\omega}$, $\mathbf{h}$,defined by

$$\omega\left(x,y\right) = \omega\left(x\left(u,v\right),y\left(u,v\right)\right) = \boldsymbol{\omega}\left(u,v\right)\ ,$$

$$\Omega\left(x,y\right) = \Omega\left(x\left(u,v\right),y\left(u,v\right)\right) = \boldsymbol{\Omega}\left(u,v\right)$$

$$h\left(x,y\right) = h\left(x\left(u,v\right),y\left(u,v\right)\right) = \mathbf{h}\left(u,v\right)\ ,$$

equation (2.8) and the system of equations (2.13)-(2.15) is replaced by the following system in the hodograph plane (u, v) :

$$\frac{\partial x}{\partial u} + \frac{\partial y}{\partial v} = 0\,, \tag{3.5}$$

$$\bar{J}\frac{\partial(\mathbf{h},y)}{\partial(u,v)} = \rho v\boldsymbol{\omega}+\kappa\bar{J}Q_1 - (\mu+\kappa)\,\bar{J}w_1 - Gu, \tag{3.6}$$

$$\bar{J}\frac{\partial(x,\mathbf{h})}{\partial(u,v)} = -\,\rho u\boldsymbol{\omega}-\kappa\bar{J}Q_2 + (\mu+\kappa)\,\bar{J}w_2 - Gv\,, \tag{3.7}$$

$$\rho j\bar{J}\left(vQ_1+uQ_2\right) = -2\kappa\boldsymbol{\Omega} + \kappa\boldsymbol{\omega} + \gamma\bar{J}\left\{\frac{\partial\left(x,\bar{J}Q_1\right)}{\partial\left(u,v\right)} + \frac{\partial\left(\bar{J}Q_2,y\right)}{\partial\left(u,v\right)}\right\}, \tag{3.8}$$

$$\bar{J}\left(\frac{\partial x}{\partial v} - \frac{\partial y}{\partial u}\right) = \boldsymbol{\omega}\,, \tag{3.9}$$

where,

$$Q_1 = Q_1(u,v) = \frac{\partial(x,\boldsymbol{\Omega})}{\partial(u,v)}\ ,\quad Q_2 = Q_2(u,v) = \frac{\partial(\boldsymbol{\Omega},y)}{\partial(u,v)}\ , \tag{3.10}$$

$$w_1 = w_1(u,v) = \frac{\partial(x,\boldsymbol{\omega})}{\partial(u,v)}\ ,\quad w_2 = w_2(u,v) = \frac{\partial(\boldsymbol{\omega},y)}{\partial(u,v)}\ . \tag{3.11}$$

System of equations (3.5) to (3.9) is a system of five equations for the five unknown functions $x(u,v), y(u,v)$, $\boldsymbol{\omega}$(u, v) ,$\boldsymbol{\Omega}(u,v)$ and $\mathbf{h}(u,v)$.

The equation of continuity implies the existence of a stream-function ψ(x, y) such that

$$d\psi = -vdx + udy \ \ or \ \ \frac{\partial \psi}{\partial x} = -v \, , \ \ \frac{\partial \psi}{\partial y} = u \ . \tag{3.12}$$

Likewise equation (3.5) implies the existence of a function L(u, v) , called the Legendre transform function of the stream-function ψ (x, y) , so that

$$dL = -ydu + xdv \ \ or \ \ \frac{\partial L}{\partial u} = -y \, , \ \ \frac{\partial L}{\partial v} = x \ , \tag{3.13}$$

and the two functions ψ (x, y)and L(u, v) are related by

$$L(u,v) = vx - uy + \psi(x,y) \, . \tag{3.14}$$

Introducing L(u, v) in the system (3.5)-(3.9), with $\bar{J}$, Q_1, Q_2, w_1, w_2, given by (3.4), (3.10) and (3.11) respectively, it follows that (3.5) is identically satisfied and the system may be replaced by

$$\bar{J}\frac{\partial\left(\frac{\partial L}{\partial u},\mathbf{h}\right)}{\partial(u,v)} = \rho v\boldsymbol{\omega} + \kappa\bar{J}Q_1 - (\mu+\kappa)\,\bar{J}w_1 - Gu, \tag{3.15}$$

$$\bar{J}\frac{\partial\left(\frac{\partial L}{\partial v},\mathbf{h}\right)}{\partial(u,v)} = -\rho u\boldsymbol{\omega} - \kappa\bar{J}Q_2 + (\mu+\kappa)\,\bar{J}w_2 - Gv\,, \tag{3.16}$$

$$\rho j\bar{J}\left(vQ_1 + uQ_2\right) = -2\kappa\boldsymbol{\Omega} + \kappa\boldsymbol{\omega} + \gamma\bar{J}\left\{\frac{\partial\left(\frac{\partial L}{\partial v},\bar{J}Q_1\right)}{\partial\left(u,v\right)} + \frac{\partial\left(\frac{\partial L}{\partial u},\bar{J}Q_2\right)}{\partial\left(u,v\right)}\right\}, \tag{3.17}$$

$$\bar{J}\left[\frac{\partial^2 L}{\partial v^2} + \frac{\partial^2 L}{\partial u^2}\right] = \boldsymbol{\omega}\,, \tag{3.18}$$

where

$$\bar{J} = \left[\frac{\partial^2 L}{\partial v^2}\frac{\partial^2 L}{\partial u^2} - \left(\frac{\partial^2 L}{\partial u \partial v}\right)^2\right]^{-1}, \tag{3.19}$$

$$Q_1 = \frac{\partial\left(\frac{\partial L}{\partial v},\boldsymbol{\Omega}\right)}{\partial(u,v)}\,, \ \ Q_2 = \frac{\partial\left(\frac{\partial L}{\partial u},\boldsymbol{\Omega}\right)}{\partial(u,v)}\,, \tag{3.20}$$

$$w_1 = \frac{\partial\left(\frac{\partial L}{\partial v},\boldsymbol{\omega}\right)}{\partial(u,v)}\,, \ \ w_2 = \frac{\partial\left(\frac{\partial L}{\partial u},\boldsymbol{\omega}\right)}{\partial(u,v)}\,, \tag{3.21}$$

By using the integrability condition

$$\left[\bar{J}\frac{\partial^2 L}{\partial u\partial v}\frac{\partial}{\partial v} - \bar{J}\frac{\partial^2 L}{\partial v^2}\frac{\partial}{\partial u}\right]\left(\bar{J}\frac{\partial\left(\frac{\partial L}{\partial u},\mathbf{h}\right)}{\partial(u,v)}\right) = \left[\bar{J}\frac{\partial^2 L}{\partial u^2}\frac{\partial}{\partial v} - \bar{J}\frac{\partial^2 L}{\partial u\partial v}\frac{\partial}{\partial u}\right]\left(\bar{J}\frac{\partial\left(\frac{\partial L}{\partial v},\mathbf{h}\right)}{\partial(u,v)}\right),$$

i.e $\partial^2 h/\partial x\partial y = \partial^2 h/\partial y \partial x$ in the (x,y) plane, we eliminate $\mathbf{h}\,(u,\ v)$ from (3.10) and (3.11) and obtain

$$-\kappa\left[\frac{\partial(\partial L/\partial v,\bar{J}Q_1)}{\partial(u,v)} + \frac{\partial(\partial L/\partial u,\bar{J}Q_2)}{\partial(u,v)}\right] + (\mu+\kappa)\left[\frac{\partial(\partial L/\partial v,\bar{J}w_1)}{\partial(u,v)} + \frac{\partial(\partial L/\partial u,\bar{J}w_2)}{\partial(u,v)}\right]$$
$$+\,G\left[\frac{\partial(\partial L/\partial v,u)}{\partial(u,v)} - \frac{\partial(\partial L/\partial u,v)}{\partial(u,v)}\right] - \rho(uw_2 + vw_1) = 0\,, \tag{3.22}$$

where $\bar{J}$, Q_1, Q_2, w_1, w_2 are given in (3.19) , (3.20) and (3.21). Summing up we have the following theorem:

Theorem 3.1. *If $L(u,\ v)$ is the Legendre transform function of a stream-function of steady, plane, incompressible, flow of an electrically conducting micropolar fluid through porous media then $L(u,\ v)$ must satisfy equation (3.17) and (3.22) where $\boldsymbol{\omega}$ $(u,\ v)$, $\bar{J}(u,\ v)$, $Q_1(u,v)$, $Q_2(u,v)$, $w_1(u,\ v)$, w_2 $(u,\ v)$ are given by (3.18), (3.19), (3.20) and (3.21).*

On finding L(u, v) and Ω(u, v), the velocity components are obtained from (3.13). Then p(x, y) and Ω(x, y) can be determined in the physical plane using the velocity components u(x, y), v(x, y).

4. Example 1

Let,

$$L\left(u,v\right)=A\left(u^2-v^2\right), \tag{4.1}$$

be the Legendre-transform function, where A is arbitrary non zero constant and. Using (4.1) in equations (3.18) -(3.21) we obtain

$$\begin{array}{ll}\bar{J}=-\frac{1}{4A^2}, & \boldsymbol{\omega}=0\,,\ w_1\left(u,v\right)=w_2\left(u,v\right)=0\\ Q_1=2A\frac{\partial\boldsymbol{\Omega}}{\partial u}, & Q_2=2A\frac{\partial\boldsymbol{\Omega}}{\partial v}\,.\end{array} \tag{4.2}$$

Using (3.15) and (3.16), in equations (3.14) and (3.12) give the following system of equations for $\boldsymbol{\Omega}$ (u,v)

$$\begin{gathered}\frac{\partial^2\boldsymbol{\Omega}}{\partial u^2}+\frac{\partial^2\boldsymbol{\Omega}}{\partial v^2}=0\,,\\ \rho j\left(u\frac{\partial\boldsymbol{\Omega}}{\partial v}+v\frac{\partial\boldsymbol{\Omega}}{\partial u}\right)=2\kappa\boldsymbol{\Omega}\,.\end{gathered} \tag{4.3}$$

Solving (4.3), we get

$$\boldsymbol{\Omega}(\mathrm{u},\mathrm{v})=\mathrm{C}_1\left(\mathrm{u}+\frac{4\mathrm{A}\kappa}{\rho\mathrm{j}}\mathrm{v}\right), \tag{4.4}$$

$$A=\frac{\rho j}{4\kappa}, \tag{4.5}$$

and $\frac{2\kappa}{\rho j}=1$, (**??**)
where C_1 is an arbitrary non-zero constant.
Using (4.1) in (3.13) and solving the resulting equations we get

$$u\left(x,y\right)=\frac{-y}{2A}\ ,\ v\left(x,y\right)=\frac{-x}{2A}\ . \tag{4.6}$$

Using (4.6) in (4.4) and (2.13), (2.14) we obtain Ω(x, y) and p(x, y) given by

$$\Omega\left(\mathrm{x},\ \mathrm{y}\right)=C_1\left(\frac{-y}{2A}-\frac{2\kappa x}{\rho j}\right), \tag{4.7}$$

$$p\left(x,\ y\right)=\kappa C_1\left(-\frac{x}{2A}+\frac{2\kappa y}{\rho j}\right)-\frac{\rho}{8A^2}\left(x^2+y^2\right)+\frac{G}{A}xy+p_\circ\ ,$$

or,

$$p\left(x,\ y\right)=\kappa C_1\left(-\frac{x}{2A}+\frac{2\kappa y}{\rho j}\right)-\frac{\rho}{8A^2}\left(x^2+y^2\right)+\frac{\left(\frac{\eta}{k}+\sigma\mathrm{B}_o^2\right)}{A}xy+p_\circ \tag{4.8}$$

,

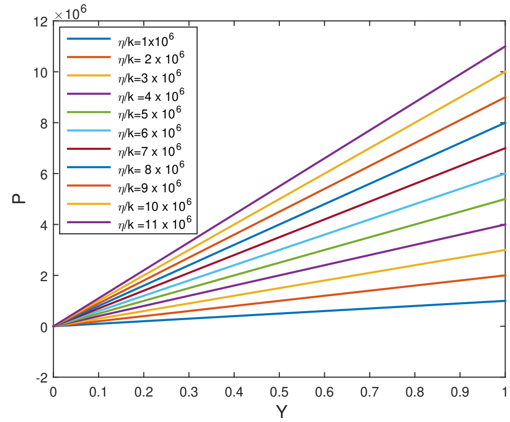

FIGURE 1. Variation of P with y at $x = 1$ for $\frac{\eta}{k}$ varying from 1×10^6 to 11×10^6 at constant $\rho = 10 \times 10^3$.

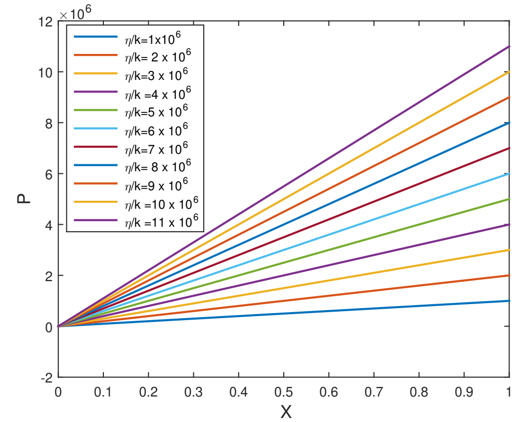

FIGURE 2. Variation of P with x at $y = 1$ for $\frac{\eta}{k}$ varying from 1×10^6 to 11×10^6 at constant $\rho = 10 \times 10^3$.

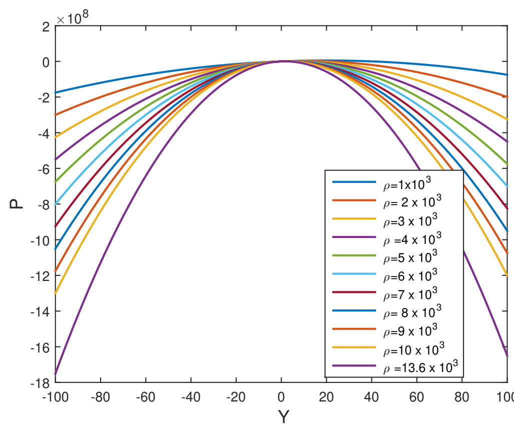

FIGURE 3. Variation of P with y at $x = 1$ for ρ varying from 10×10^3 to 13.6×10^3 at constant $\frac{\eta}{k} = 5 \times 10^6$.

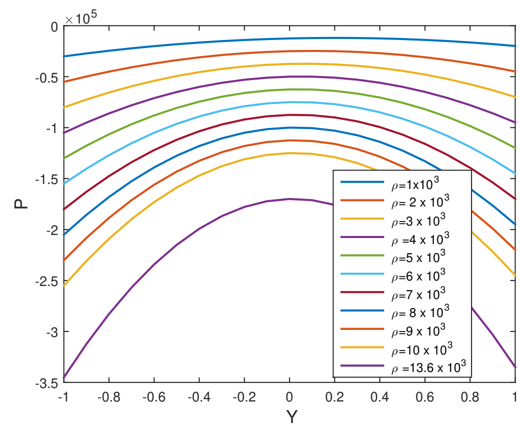

FIGURE 4. Variation of P with y at $x = 1$ for ρ varying from 10×10^3 to 13.6×10^3 at constant $\frac{\eta}{k} = 5 \times 10^4$.

And the streamlines are given by $x^2 - y^2 = Constant$. This shows that the streamlines of the flow equations are concentric hyperbolas.

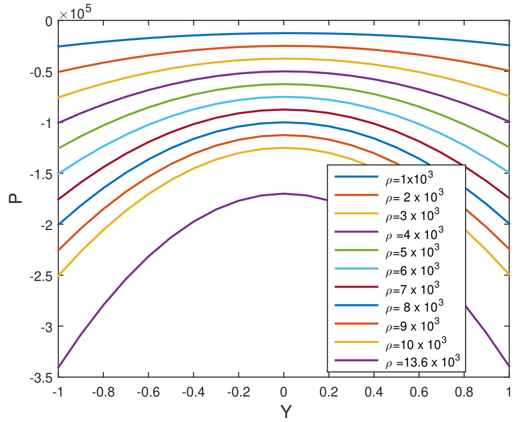

FIGURE 5. Variation of P with y at $x = 1$ for ρ varying from 10×10^3 to 13.6×10^3 at constant $\frac{\eta}{k}= 5 \times 10^3$.

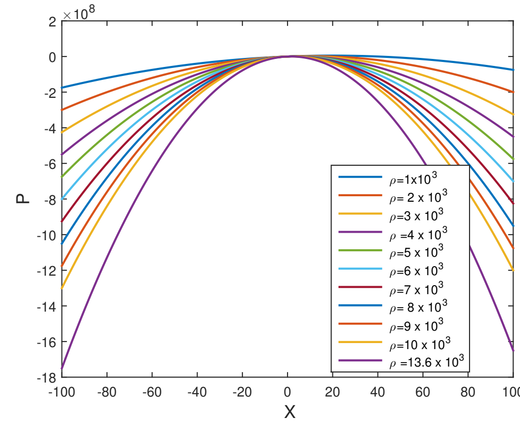

FIGURE 6. Variation of P with x at $y = 1$ for ρ varying from 10×10^3 to 13.6×10^3 at constant $\frac{\eta}{k}$=5×10^6.

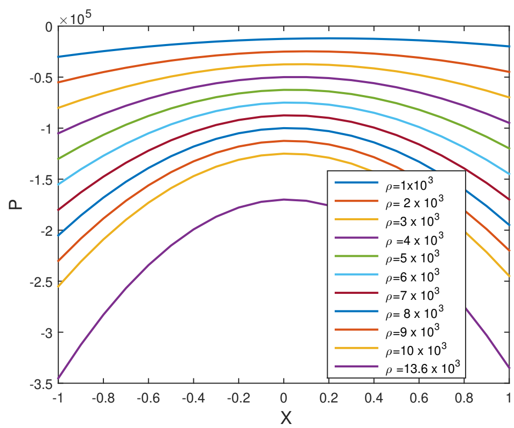

FIGURE 7. Variation of P with x at $y = 1$ for ρ varying from 10×10^3 to 13.6×10^3 at constant $\frac{\eta}{k}= 5 \times 10^4$.

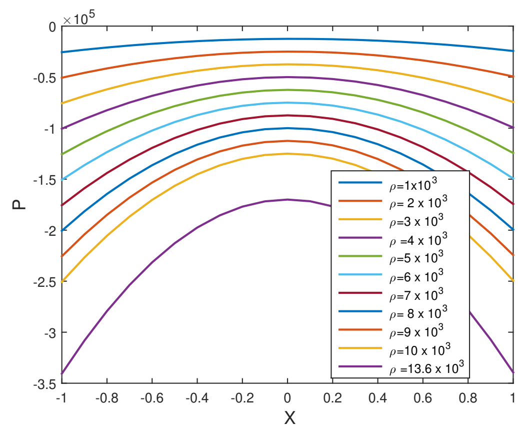

FIGURE 8. Variation of P with x at $y = 1$ for ρ varying from 10×10^3 to 13.6×10^3 at constant $\frac{\eta}{k}$=5×10^3.

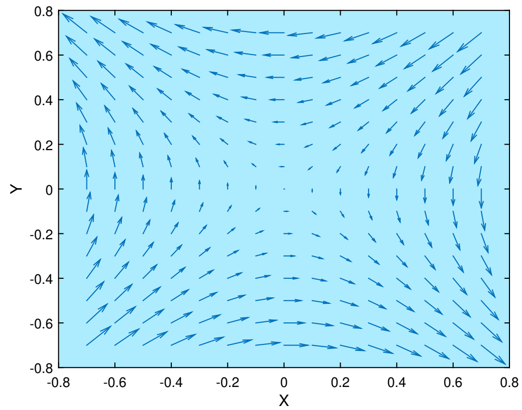

FIGURE 9. Streamlines for $x^2 - y^2 = Constant$.

Theorem 4.1. *If $L(u,v) = A(u^2 - v^2)$ is the Legendre transform function of a stream function for steady, plane, incompressible, flow of an electrically conducting micropolar fluid through porous media, then the flow in the physical plane is a flow with concentric hyperbolic streamlines with flow variables given by (4.6), (4.7) and (4.8).*

5. EXAMPLE 2

Let,

$$L(u,v) = uv, \tag{5.1}$$

be the Legendre- transform function.
Using (5.1) in (3.18)-(3.21), we find that

$$\begin{aligned} &L(u,v) = uv\ , \\ &\bar{J} = -1\ ,\ \ \boldsymbol{\omega} = 0\ ,\ w_1 = w_2 = 0\ , \\ &Q_1 = \tfrac{\partial \boldsymbol{\Omega}}{\partial v},\quad Q_2 = -\tfrac{\partial \boldsymbol{\Omega}}{\partial u}\quad . \end{aligned} \tag{5.2}$$

Using (5.1) and (5.2) in equations (3.22) and (3.17)

$$\begin{aligned} \frac{\partial^2 \boldsymbol{\Omega}}{\partial u^2} + \frac{\partial^2 \boldsymbol{\Omega}}{\partial v^2} &= 0\,, \\ \rho j\left(v\frac{\partial \boldsymbol{\Omega}}{\partial v} - u\frac{\partial \boldsymbol{\Omega}}{\partial u}\right) &= 2\kappa \boldsymbol{\Omega}\,. \end{aligned} \tag{5.3}$$

Solving these equations , we get

$$\boldsymbol{\Omega}(\mathrm{u},\mathrm{v}) = C_2 v, \tag{5.4}$$

$$\frac{2\kappa}{\rho j} = 1, \tag{5.5}$$

where C_2 is an arbitrary constant.
On proceeding as in Example 1, we get

$$u(x,\,y) = x\ ,\qquad v(x\,,y) = -y\ , \tag{5.6}$$

$$\Omega(\mathrm{x},\ \mathrm{y}) = -C_2 y, \tag{5.7}$$

and

$$p(x,\,y) = -C_2\kappa x - \frac{G}{2}\left(x^2 - y^2\right) - \frac{1}{2}\rho\left(x^2 + y^2\right) + p_1\ ,$$

or,

$$p(x,\,y) = -C_2\kappa x - \frac{\left(\frac{\eta}{k} + \sigma \mathrm{B}_o^2\right)}{2}\left(x^2 - y^2\right) - \frac{1}{2}\rho\left(x^2 + y^2\right) + p_1, \tag{5.8}$$

where p_1 is an arbitrary constant.
And the streamlines are given by $yx = Constant$.
This shows that the streamlines of the flow equations are rectangular hyperbolae.

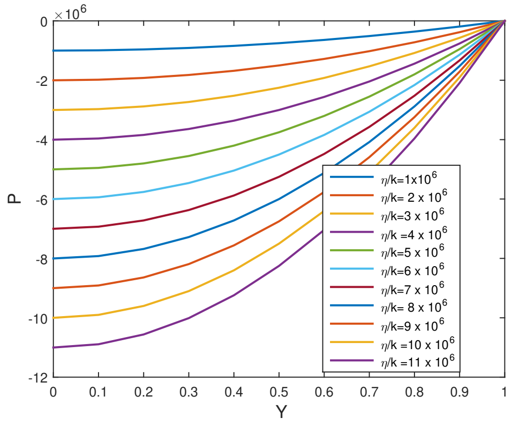

FIGURE 10. Variation of P with y from 0 to 1 at $x = 1$ for $\frac{\eta}{k}$ varying from 1×10^6 to 11×10^6 at constant $\rho = 12 \times 10^3$.

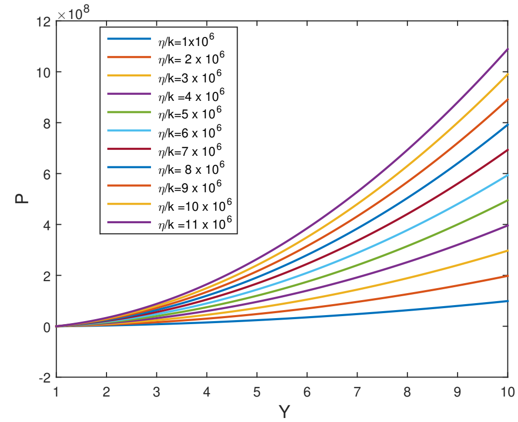

FIGURE 11. Variation of P with y from 1 to 10 at $x = 1$ for $\frac{\eta}{k}$ varying from 1×10^6 to 11×10^6 at constant $\rho = 12 \times 10^3$.

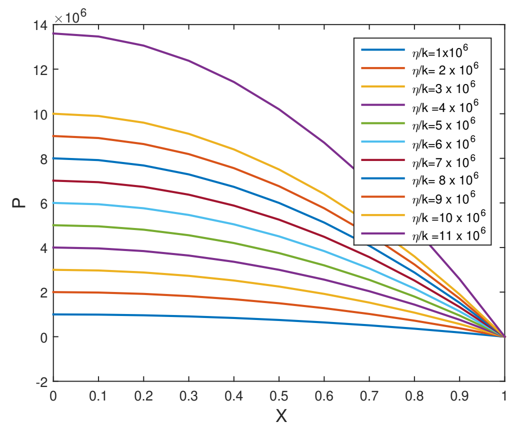

FIGURE 12. Variation of P with x from 0 to 1 at $y = 1$ for $\frac{\eta}{k}$ varying from 1×10^6 to 11×10^6 at constant $\rho = 12 \times 10^3$.

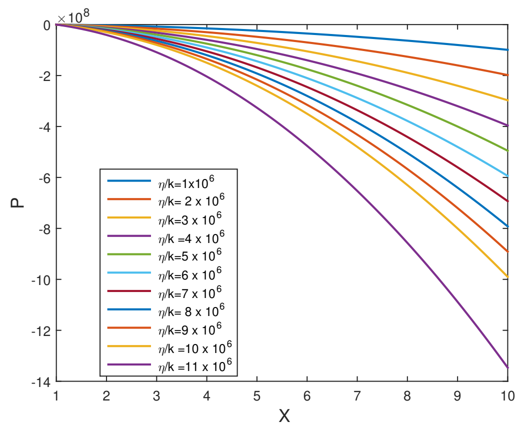

FIGURE 13. Variation of P with x from 1 to 10 at $y = 1$ for $\frac{\eta}{k}$ varying from 1×10^6 to 11×10^6 at constant $\rho = 12 \times 10^3$.

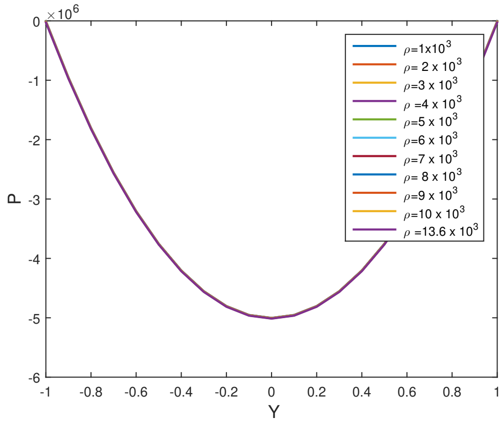

FIGURE 14. Variation of P with y at $x = 1$ for ρ varying from 10×10^3 to 13.6×10^3 at constant $\frac{\eta}{k} = 5 \times 10^6$.

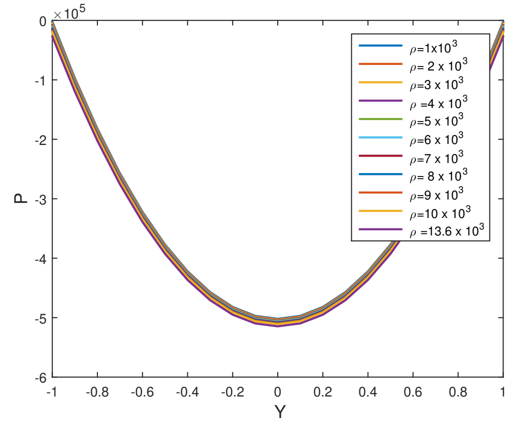

FIGURE 15. Variation of P with y at $x = 1$ for ρ varying from 10×10^3 to 13.6×10^3 at constant $\frac{\eta}{k} = 5 \times 10^5$.

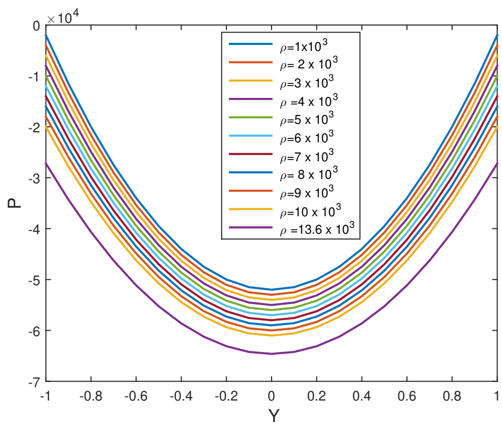

FIGURE 16. Variation of P with y at $x = 1$ for ρ varying from 10×10^3 to 13.6×10^3 at constant $\frac{\eta}{k} = 5 \times 10^4$.

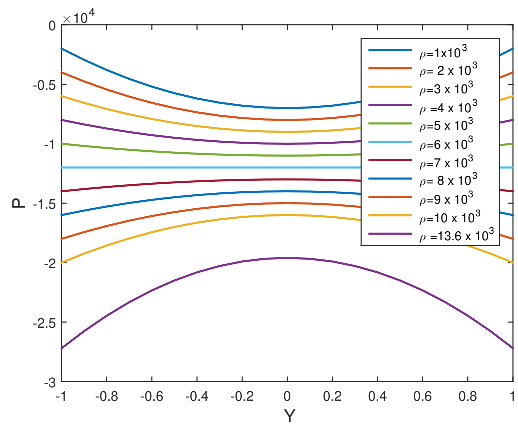

FIGURE 17. Variation of P with y at $x = 1$ for ρ varying from 10×10^3 to 13.6×10^3 at constant $\frac{\eta}{k} = 5 \times 10^3$.

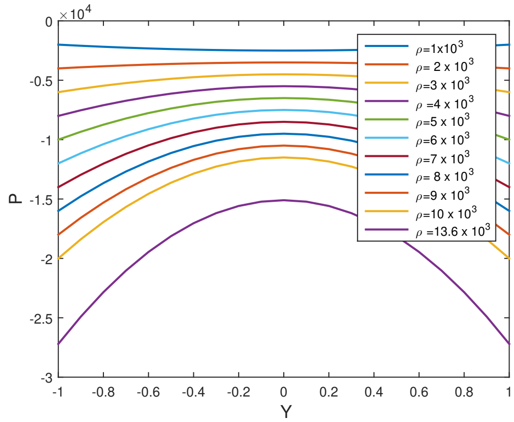

FIGURE 18. Variation of P with y at $x = 1$ for ρ varying from 10×10^3 to 13.6×10^3 at constant $\frac{\eta}{k} = 5 \times 10^2$.

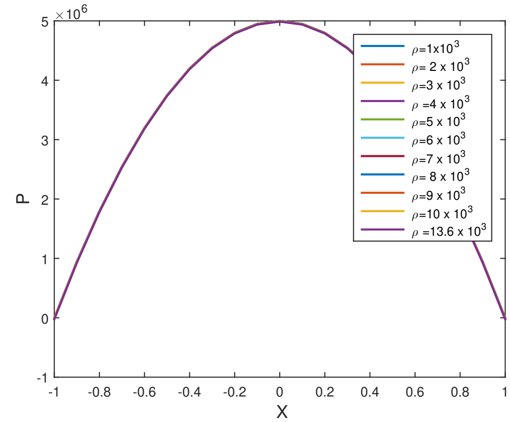

FIGURE 19. Variation of P with x at $y = 1$ for ρ varying from 10×10^3 to 13.6×10^3 at constant $\frac{\eta}{k} = 5 \times 10^6$.

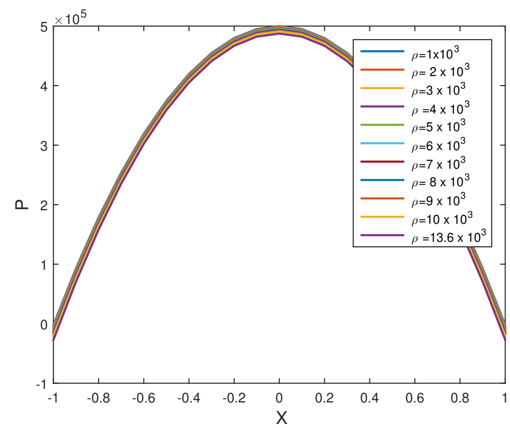

FIGURE 20. Variation of P with x at $y = 1$ for ρ varying from 10×10^3 to 13.6×10^3 at constant $\frac{\eta}{k} = 5 \times 10^5$.

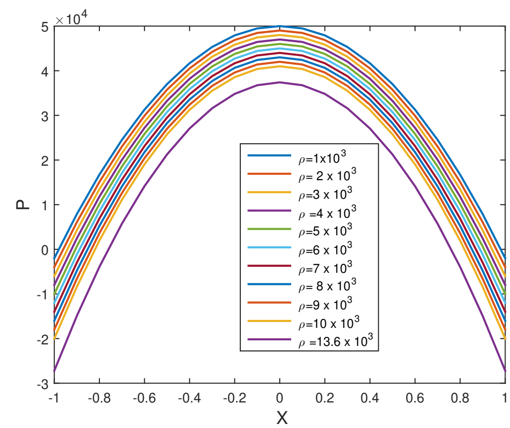

FIGURE 21. Variation of P with x at $y = 1$ for ρ varying from 10×10^3 to 13.6×10^3 at constant $\frac{\eta}{k} = 5 \times 10^4$.

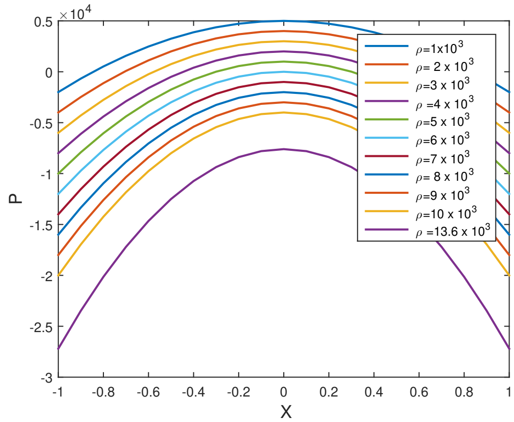

FIGURE 22. Variation of P with x at $y = 1$ for ρ varying from 10×10^3 to 13.6×10^3 at constant $\frac{\eta}{k} = 5 \times 10^3$.

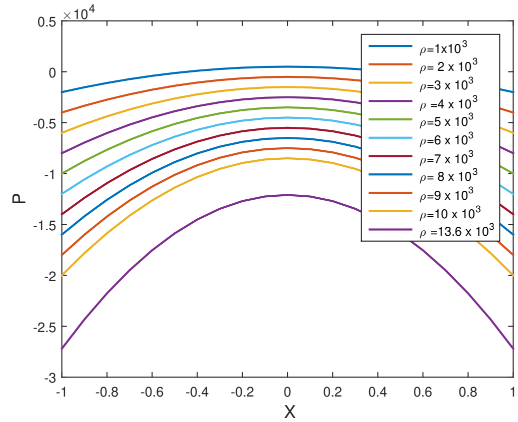

FIGURE 23. Variation of P with x at $y = 1$ for ρ varying from 10×10^3 to 13.6×10^3 at constant $\frac{\eta}{k} = 5 \times 10^2$.

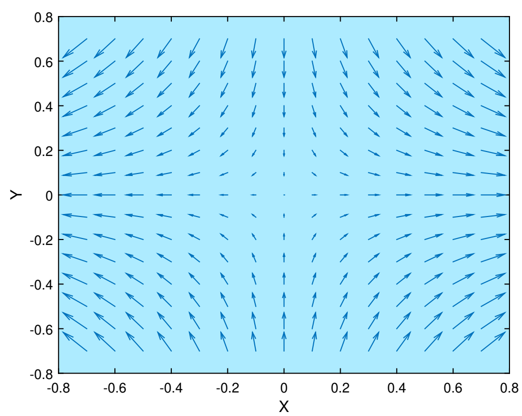

FIGURE 24. Streamlines for $yx = Constant$.

Theorem 5.1. *If $L(u,v) = uv$ be the Legendre transform function of a stream function for steady, plane, incompressible, flow of an electrically conducting micropolar fluid through porous media, then the flow in the physical plane is a flow with rectangular hyperbolae streamlines with flow variables given by* (5.6)*,* (5.7) *and* (5.8)*.*

6. Main results

In this paper, an approach has been carried out where hodograph transformation method has been applied for the exact solution of the equations governing the flow through porous media of a micropolar fluid which is electrically conducting. Two different forms of Legendre transform function of the stream function have been considered as examples to illustrate the technique of solving for the exact solution. The expressions for velocity components, micro-rotation and pressure distribution are found out in each case. The main results of the present work is listed below:

(1) In example 1 the streamlines are given by $x^2 - y^2 = constant$ and the vorticity is zero. The solutions for the components of velocity, microrotation and pressure are given by equations (4.6), (4.7) and (4.8) respectively.
(2) In example 2 we see that the streamlines are given by $yx = constant$ and the vorticity is zero. In this example the components of velocity, microrotation and pressure are given by equations (5.6), (5.7) and (5.8) respectively.
(3) The Streamline patterns are plotted in each case. In example 1 the streamlines are found to be concentric hyperbolas shown in figure 9 and in example 2 the streamlines are rectangular hyperbolae as seen in figure 24.
(4) For each examples the pressure variation with y keeping $x = 1$ and pressure variation with x keeping $y = 1$ are plotted for varying porous media parameter $\frac{\eta}{k}$ (permeability of the medium is varied) at constant density $\rho$and also for varying density ρ of different fluids at constant $\frac{\eta}{k}$ value.
(5) In example 1:
   - It is evident that the pressure increases linearly with y as well as x for varying $\frac{\eta}{k}$ at constant density ρ in figure 1 and 2. The rate of change in pressure with respect to $y$or$x$ increases with increase in $\frac{\eta}{k}$.
   - For varying density ρ at constant $\frac{\eta}{k}$ there is a inverted parabolic variation of pressure which is symmetric about $y = 0$ or $x = 0$ as observed in figure 3and figure 6. The width of the inverted parabola is seen to be narrowing with increasing ρ. Also, the inverted parabola seems to flatten if the value of $\frac{\eta}{k}$ is decreased as in figure 4, figure 5, figure 7 and figure 8.
(6) In example 2:
   - From figure 10 and figure 11, it is observed that pressure increases with y for varying $\frac{\eta}{k}$ at constant density ρ, converging at $y = 1$ and goes on increasing with similar manner. The rate of change in pressure with respect to y increases with increase in $\frac{\eta}{k}$. From figure 12 and figure 13, it is clear that pressure decreases with x for varying

$\frac{\eta}{k}$ at constant density ρ with pressure value converging at $x = 1$ and further decreases with a similar way. The rate of change in pressure with respect to $y$increases with increase in $\frac{\eta}{k}$.

- For fluids of different density ρ at constant $\frac{\eta}{k}$ there is a parabolic variation of pressure with $y$which is symmetric about $y = 0$ as can be seen in figure 14, figure 15 and figure 16. For higher values of $\frac{\eta}{k}$, the plots for different ρ overlaps with each other and a single curve is observed (figure 14). On decreasing the values of $\frac{\eta}{k}$, different curves are obtained and width of parabola becomes wider with increasing ρ in figure 15 and figure 16. On further decreasing the value $\frac{\eta}{k}$ the parabolas seem to invert and the extent of inversion is most prominent for higher ρvalues (figure 17 and figure 18). As observed in figure 19, the pressure variation with x for different density ρ at constant $\frac{\eta}{k}$, is inverted parabolic, symmetric about $x = 0$with the variation overlapping for any value of density for higher $\frac{\eta}{k}$ value. And from figure 20, figure 21, figure 22 and figure 23, it can be seen that on decreasing the value of $\frac{\eta}{k}$ the curves for different ρgets separated with the width of the inverted parabola found to become narrower with increasing ρ.

The present analysis is more general and results of Indrasena [2] and Sayantan Sil & Manoj Kumar [54] can be recovered in the limiting cases.

Acknowledgement. The author is grateful to Dr. Manoj Kumar, his P.hD. supervisor and Mr. Birendra Kumar Vishwakarma, his research scholar for their useful and valuable suggestions which contributed to the completion of this work.

References

1. Abdel-Rahman, G. M. (2011). Effect of Magnetohydrodynamic on Thin Films of Unsteady Micropolar Fluid through a Porous Medium. Journal of Modern Physics, 2(11), 1290-1304. https://doi.org/10.4236/jmp.2011.211160
2. Adluri, I. (1995). Hodographic study of plane micropolar fluid flows. Int. J. Math. & Math. Sci., 18(5), 357-364. https://doi.org/10.1155/S0161171295000445
3. Ahmadi, G., & and Shahinpoor, M. (1974). Universal stability of magneto-micropolar fluid motions. International Journal of Engineering Science, 12(7), 657-663. https://doi.org/10.1016/0020-7225(74)90042-1
4. Ames, W. F. (1965). Non-lineaEngineeringr partial differential equations in . New York: Academic Press. https://doi.org/10.1002/aic.690120239
5. Barron, R., & Chandna, O. P. (1981). Hodograph transformation and solutions in constantly inclined MHD plane flows. J. Engg. Math., 15(3), 211-220. https://doi.org/10.1007/BF00042781
6. Bhatt, B., & Shirley, A. (2008). Plane viscous flows in porous medium. Matematicas: Ensenanza Universitaria, XVI(1), 51-62.
7. Borrelli, A., G, G., & Patria, M. C. (2015). An exact solution for the 3D MHD stagnation-point flow of a micropolar fluid. Communications in Nonlinear Science and Numerical Simulation, 20(1), 121-135. https://doi.org/10.1016/j.cnsns.2014.04.011
8. Borrelli, A., Giantesio, G., & Patria, M. C. (2011). Three-dimensional MHD stagnation point-flow of a Newtonian and a micropolar fluid. International Journal of Pure and Applied Mathematics, 73(2), 165-188.

9. Borrelli, A., Giantesio, G., & Patria, M. C. (2012). MHD oblique stagnation-point flow of a micropolar fluid. Applied Mathematical Modelling, 36(9), 3949-3970. https://doi.org/10.1016/j.apm.2011.11.004
10. Borrelli, A., Giantesio, G., & Patria, M. C. (2013). Numerical simulations of three-dimensional MHD stagnation-point flow of a micropolar fluid, Computers & Mathematics with Applications, 66(4), 472-489. https://doi.org/10.1016/j.camwa.2013.05.023
11. Borrelli, A., Giantesio, G., & Patria, M. C. (2015). An exact solution for the 3D MHD stagnation-point flow of a micropolar fluid. Communications in Nonlinear Science and Numerical Simulation, 20(1), 121-135. https://doi.org/10.1016/j.cnsns.2014.04.011
12. Borrelli, A., Giantesio, G., & Patria, M. C. (2015). Influence of a non-uniform external magnetic field on the oblique stagnation-point flow of a micropolar fluid. Journal of Applied Mathematics, 80(3), 747-765. https://doi.org/10.1093/imamat/hxu019
13. Borrelli, A., Giantesio, G., & Patria, M. C. (2015). MHD orthogonal stagnation-point flow of a micropolar fluid with the magnetic field parallel to the velocity at infinity. (2015). Applied Mathematics and Computation, 264, 44-60. https://doi.org/10.1016/j.amc.2015.04.058
14. Chandna, O. P., & Garg, M. (1979). On steady plane magnetohydrodynamic flows with orthogonal magnetic and velocity field. Int. J. Engg. Sci., 17, 251-257. https://doi.org/10.1016/0020-7225(79)90088-0
15. Chandna, O. P., Barron, R., & Chew, K. (1982). Hodograph transformations and solutions in variably inclined MHD plane flows. J. Engg. Math., 16(3), 223-243. https://doi.org/10.1007/BF00042718
16. Chandna, O.P., Barron, R., & Smith. (1982). Rotational plane flows of a viscous fluid. SIJM. J. Appl. Math., 42, 1323-1336. https://doi.org/10.1137/0142092
17. Chandna, O.P., & Nguyen, P. (1989). Hodograph method in non-Newtonian MHD transverse fluid flows. J. of Engg. Math., 23, 119-139. https://doi.org/10.1007/BF00128864
18. Chen, M., Huang, B., & Zhang, J. (2013). Blowup criterion for the three-dimensional equations of compressible viscous micropolar fluids with vacuum . Nonlinear Analysis: Theory, Methods & Applications, 79 , 1-11. https://doi.org/10.1016/j.na.2012.10.013
19. Cherry, T. M. (1959). Some nozzle flows found by the hodograph method. Journal of the Australian Mathematical Society, 1(1), 80–94. https://doi.org/10.1017/S144678870002509X
20. Eringen, A.C. (1966). Theory of micropolar fluids. J.Math.Mech., 16, 1-18.
21. Eringen, A. C. (1964). Simple microfluids. Int. Engng.Sci., 2, 205-217. https://doi.org/10.1016/0020-7225(64)90005-9
22. Eringen, A. C. (1966). Mechanics of micromorphic materials. In Applied Mechanics: Proceedings of the Eleventh International Congress of Applied Mechanics Munich (Germany) 1964 (pp. 131-138). Springer Berlin Heidelberg. https://doi.org/10.1007/978-3-662-29364-5_12
23. Ghaffari, A. G., & Temple, G. (1950). The hodograph method in gas dynamics.Tehran: Taban Press.
24. Hayat, T., & Ali, N. (2008). Effects of an endoscope on peristaltic flow of a micropolar fluid. Mathematical and Computer modelling, 18, 721-733. https://doi.org/10.1016/j.mcm.2007.11.004
25. Hussain, M., Ashraf, M., Nadeem, S., & Khan, M. (2013). Radiation effects on the thermal boundry layer flow of a micropolar fluid towards a permeable stretching sheet. Journal of the Franklin Institute, 350, 194-210. https://doi.org/10.1016/j.jfranklin.2012.07.005
26. Hussain, S., Kamal, M. A., & Ahmad, F. (2014). The acclerated rotating disk in a micropolar fluid flow. Appl.Math.Mech., 5, 196-202. https://doi.org/10.4236/am.2014.51020
27. Ingham, D.B., & Poop, I. (1998). Transport Phenomena in Porous Media,. Elsevier. https://doi.org/10.1016/B978-0-08-042843-7.X5000-4

28. Ishak, A., Nazar, R., & Pop, I. (2008). Magnetohydrodynamic (MHD) flow and heat transfer due to a stretching cylinder. Energy Conversion and Management, 9(11), 3265-3269. https://doi.org/10.1016/j.enconman.2007.11.013
29. Jamal, M., & Arsalan, A. (2020). New travelling wave solutions of MHD micropolar fluid in porous medium. Journal of Egyptian Mathematical Society, 28 (1), 1-22. https://doi.org/10.1186/s42787-020-00085-5
30. Kasiviswanathan, S. R., & Gandhi, M. V. (1992). A class of exact solutions for the magnetohydrodynamic flow of a micropolar fluid. International journal of engineering science, 30(4), 409-417. https://doi.org/10.1016/0020-7225(92)90033-D
31. Khalid, A., Khan, I., Khan, A., & Shafie, S. (2018). Influence of wall couple stress in MHD flow of a micropolar fluid in a porous medium with energy and concentration transfer. Results in Physics, 9, 1172-1184. https://doi.org/10.1016/j.rinp.2018.04.005
32. Kocić, M, Stamenković, Ž., Petrović, J., & Bogdanović-Jovanović, J. (2023). MHD micropolar fluid flow in porous media. Advances in Mechanical Engineering, 15(6), 1-18. https://doi.org/10.1177/168781322311784
33. Kumar, M. (2014). Solution of non-Newtonian fluid flows through porous media by hodograph transformation method. Bull. Cal. Math. Soc., 106(4), 239-250.
34. Kumar, M., Sil, S., & Prajapati, M. (2018). Rotating MHD flow: An exact solution by hodograph transformation. Bulletin of Pure & Applied Sciences-Physics, 37(2), 88-107. https://doi.org/10.5958/2320-3218.2018.00014.3
35. Kumar, M., Sil, S., & Prajapati, M. (2022). Exact Solutions of non-Newtonian Fluid of Rotating MHD Flows Through Porous Media with Hall Effect by Complex Variable Technique. Gulf Journal of Mathematics, 12(2), 66-73. https://doi.org/10.56947/gjom.v12i2.789
36. Kumar, M., Sil, S., & Thakur, C. (2013). Hodograph transformation in constantly inclined two phase MFD flows through porous media. International Journal of Mathematical Archive, 4(7), 42-47.
37. Kumar, M., Sil, S., & Thakur, C. (2014). Some exact solutions for the flow of second grade MHD Fluid Via Prescribed Vorticity. Acta Ciencea Indica, 40(1), 123-133.
38. Kumar, M., Sil, S., & Thakur, C. (2015). Inverse solutions for Unsteady Second Grade Aligned MHD Fluid Flow Through Porous Media. Bull. Cal. Math. Soc., 107(2), 179-192.
39. Kumaran, G., Sivaraj, R., Prasad, V. R., Beg, O. A., Leung, H. H., & Kamalov, F. (2021). Numerical study of axisymmetric magneto-gyrotactic bioconvection in non-Fourier tangent hyperbolic nano-functional reactive coating flow of a cylindrical body in porous media. The European Physical Journal Plus, 136(11), 1107. https://doi.org/10.1140/epjp/s13360-021-02099-z
40. Łukaszewicz, G. (1999). Micropolar Fluids Theory and Applications. Birkhäuser.
41. Majidian, A., Parvizi, O. M., Amani, A., Golipour, M., Bazgir, H. B., & Domairry, G. (2015). An Analytical Solution for MHD Micro Polar Fluid Transport Phenomena over a Stretching Permeable Sheet. International Journal of Basic & Applied Sciences, 15(1), 11-19.
42. Mishra, P., & Mishra, R. (2010). Hodograph transformations in unsteady MHD transverse flows. Applied Mathematical Sciences, 56(4), 2781-2795.
43. Mohyuddin, M., Siddiqui, A., Hayat, T., Siddiqui, J., & Asghar, S. (2008). Exact solutions of time dependent Navier-Stokes equations by Hodograph-Legendre transformation method. Tamsui Oxford Journal of Mathematical Sciences, 24(3), 257-268.
44. Moro, L., Siddiqui, A., & Kaloni, P. (1990). Steady flows of a third-grade fluid by transformation methods. ZAMM, 70, 189-198. https://doi.org/10.1002/zamm.19900700309
45. Prajapati, M., Sil, S., & Kumar, M. (2018). A Class of Exact Solutions of MHD Fluid through Porous Media with Variable Permeability using Inverse Method. Bulletin of Calcutta Mathematical Society, 110(4), 333-354.
46. Ram, G., & Mishra, R. (1977). Unsteady MHD flow of fluid through porous medium in a circular pipe. Ind. J. Pure and Appl. Math., 8(6), 637-647.

47. Rashad, A. M. (2014). 2014. Effects of radiation and variable viscosity on unsteady MHD flow of a rotating fluid from stretching surface in porous medium.,Journal of the Egyptian Mathematical Society, 22(1), 134-142. https://doi.org/10.1016/j.joems.2013.05.008
48. Santhosh, N., Sivaraj, R., Ramachandra Prasad, V., Anwar Bég, O., Leung, H. H., Kamalov, F., & Kuharat, S. (2023). Computational study of MHD mixed convective flow of Cu/Al2O3-water nanofluid in a porous rectangular cavity with slits, viscous heating, Joule dissipation and heat source/sink effects. Waves in Random and Complex Media, 1-34. https://doi.org/10.1080/17455030.2023.2168786
49. Shahzad, F., Sajid, M., Hayat, T., & M, A. (2006). Analytic solutions for flow of a micropolar fluid. Acta Mechanica, 188, 93-102. https://doi.org/10.1007/s00707-006-0398-4
50. Sheikh, N., Ali, F., Khan, I., Saqib, M., & Khan, A. (2017). MHD flow of micropolar fluid over an oscillating vertical plate embedded in porous media with constant temperature and concentration. Mathematical Problems in Engineering, 1-20. https://doi.org/:10.1155/2017/9402964
51. Siddiqui, A., Kaloni, P., & Chandna, O. (1985). Hodograph transformation methods in non-Newtonian fluids. J. of Engg. Math, 19, 203-216.
52. Sil, S., & Kumar, M. (2014). A Class of solution of orthogonal plane MHD flow through porous media in a rotating frame. Global Journal of Science Frontier Research: A Physics and Space Science, 14(7), 17-26.
53. Sil, S., & Kumar, M. (2015). Exact solution of second grade fluid in a rotating frame through porous media using hodograph transformation method. J. Appl. Math. Phys. , 3, 1443-1453. https://doi.org/10.4236/jamp.2015.311172
54. Sil, S., & Kumar, M. (2019). Plane Micropolar Fluid Through a Porous Medium: Exact Solution by Hodograph Transformation. International Journal of Applied Engineering Research, 14(12), 2824-2829.
55. Sil, S., Kumar, M., & Singh, S. (2018). Solution of Constantly Inclined Rotating Two Phase Magnetohydrodynamic Flows Through Porous Media. International Journal of Mathematical Archive, 9(3), 225-231.
56. Sil, S., Kumar, M., & Thakur, C. (2012). Solutions of non-Newtonian MHD transverse fluid flows through porous media. Proceedings of 57th Congress of ISTAM, An International Meet, (pp. 13-21). Defence Institute of Advanced Technology, Pune, India.
57. Sil, S., Prajapati, M., & Kumar, M. (2022). A Magnetographic analysis Of MHD orthogonal rotating flow. Advances and Applications in Mathematical Sciences, 22(2), 367-377.
58. Sil, S., Vishwakarma, B. K., & Kumar, M. (2021). Analytical solutions of second grade electrically conducting fluid with Hall Effect through porous media using hodograph transformation. Ganita, 71(2), 81-98.
59. Singh, H., & Mishra, R. (1987). Legendre transformation in steady plane MHD flows of a viscous fluid. Indian J. of Pure and Appl. Math., 18(1), 100-109.
60. Singh, K. K., & Singh, D. P. (1993). Steady plane MHD flows through porous media with constant speed along each stream line. Bulletin of Calcutta Mathematical Society, 85(3), 255-262.
61. Singh, S., & Tripathi, D. (1987). Hodograph transformations in steady plane rotating MHD flows. Applied Scientific research, 43, 347-353.
62. Srinivasacharya, D., & Shiferaw, M. (2008). Numerical solution to the MHD flow of micropolar fluid between parallel porous plates. International Journal of Fluid Mechanics Research, 35(4), 365-373. https://doi.org/10.1615/InterJFluidMechRes.v35.i4.60
63. Srinivasacharya, D., & Shiferaw, M. (2010). Magnetohydrodynamic flow of a micropolar fluid in a circular pipe with Hall effects. The ANZIAM Journal , 51(2), 277-285. https://doi.org/10.21914/anziamj.v51i0.1835
64. Sumithra, A., Sivaraj, R., Prasad, V. R., Bég, O. A., Leung, H. H., Kamalov, F., ... & Kumar, B. R. (2023). Computation of inclined magnetic field, thermophoresis and Brownian motion effects on mixed convective electroconductive nanofluid flow in a rectangular porous

enclosure with adiabatic walls and hot slits. International Journal of Modern Physics B, 2450398. https://doi.org/10.1142/S0217979224503983

65. Swaminathan, M., Chandna, O. P., & Sridhar, K. (1983). Hodograph study of transverse MHD flows. Canadian J. of Physics, 61, 1323-1336. https://doi.org/10.1139/p83-134
66. Thakur, C., & Mishra, R. (1988). On steady plane rotating hydromagnetic flows. Astrophysics and Space Science, 146(1), 89-97. https://doi.org/10.1007/BF00656985
67. Thakur, C., & Singh, B. (2000). Study of variably inclined MHD flows through porous media in magnetograph plane. Bull. Cal. Math. Soc., 92, 39-50.
68. Thakur, C., Kumar, M., & Mahan, M. (2006). Exact solution of steady MHD orthogonal plane fluid flows through porous media. Bull. Cal. Math. Soc., 98(6), 583-596.
69. Vishwakarma, B. K., Sil, S., & Kumar, M. (2022). Exact solution of unsteady transverse MHD flow in rotating frame by hodograph transformation. Bulletin of Calcutta Mathematical Society, 114(4), 461-488.
70. Xu, F. (2012). Regularity criterion of weak solutions for the 3D Magneto-micropolar fluid equations in Besov spaces. Communications in Nonlinear Science and Numerical Simulation, 17(6), 2426-2433. https://doi.org/10.1016/j.cnsns.2011.09.038

Department of Physics, P.K. Roy Memorial College, Dhanbad-826004, BBMK University, Dhanbad, Jharkhand, India.

Email address: sayan12350@gmail.com